Eur. Phys. J. D **20**, 27–36 (2002)
DOI: 10.1140/epjd/e2002-00113-4

THE EUROPEAN PHYSICAL JOURNAL D

Long-range atom-metal-surface interaction and interference of atomic states

Yu.L. Sokolov[1,a], V.P. Yakovlev[2,b], V.G. Pal'chikov[3,c], and Yu.A. Pchelin[1]

[1] Russian Research Center "Kurchatov Institute" OGRA, 123182 Moscow, Russia
[2] Moscow Engineering Physics Institute, 115409 Moscow, Russia
[3] National Research Institute for Physical-Technical and Radiotechnical Measurements, VNIIFTRI, Mendeleevo, 141570 Moscow Region, Russia

Received 9 January 2002 / Received in final form 8 April 2002
Published online 28 June 2002

Abstract. The effect of long-range interaction of metastable hydrogen atoms with a metal surface is experimentally studied. The suggested experimental scheme uses the interaction as a component of an atomic interferometer. Qualitative and quantitative estimates of the atom-surface interaction are obtained for various experimental designs.

PACS. 31.30.Jv Relativistic and quantum electrodynamic effects in atoms and molecules – 32.70.Fw Absolute and relative intensities – 39.10.+j Atomic and molecular beam sources and techniques – 39.20.+q Atom interferometry

1 Introduction

Precision studies of simple quantum systems like hydrogen and hydrogen-like atoms [1] have been one of the most important sources of fundamental physical information. This is due to an impressive recent progress in quantum technology and experimental technique, which often challenges the current theoretical notions.

In the paper we present a detailed experimental study of the long-range interaction of metastable hydrogen atoms with metallic surfaces reported earlier in references [2–4].

The metastable hydrogen 2S-state decays in two photons ($2E1$) with a life-time of 1/8 229 s [5,6]. In an external dc electric field, the Stark mixing of 2S and 2P states occurs and the radiative life-time of the 2S-state significantly decreases due to the dipole transition to the ground state induced by the external field. The induced decay rate is proportional to the square of the electric field amplitude. Different aspects of this process were studied in detail from various points of view, in particular to test the applicability of Bethe-Lamb theory [7]. The peculiarities in angular distribution and anisotropy of hydrogen emission in the external field were studied theoretically and experimentally in [8–15].

A distinctive feature of our method [16] is the observation of the interference of $2S_{1/2}$ (or $2P_{1/2}$) states in a wide range of the phase shifts. This allows, for example, the measurement of the Lamb shift with a high accuracy [17–19].

In the paper the process of interaction of a hydrogen atom with a metal surface is used as a part of the scheme of an atomic interferometer. This is the key point of our experiments because of the interference pattern is very sensitive to small perturbation of its components [16], therefore this scheme turns out to be a convenient tool for precision studies of long-range interactions of metastable hydrogen atoms with metal surfaces.

2 The interference of atomic states

We recall the basic principles [16] of observation of the interference of $2S_{1/2}$ (or $2P_{1/2}$) states of atomic hydrogen states, as illustrated in Figure 1.

A beam of metastable $2S_{1/2}$ hydrogen atoms crosses the electric field E, which sharply (non-adiabatically) drops at the boundaries 1 and 2. After crossing boundary 1, the atoms pass into the superposition of eigenstates φ_1 and φ_2 with energies ε_1 and ε_2, respectively, which essentially depend on the field strength due to the Stark effect. At the boundary 2, where the field vanishes, each of the states φ_1 and φ_2 should be considered as a superposition of eigenstates $2S_{1/2}$ and $2P_{1/2}$ in the field-free space. So the resulting amplitude of these states will contain phase-shifted contributions $(2S)_1-(2S)_2$ and $(2P)_1-(2P)_2$ from the states φ_1 and φ_2, respectively, which evolved along different "paths" before. The value of the shift $(\varepsilon_1 - \varepsilon_2)T/\hbar$ depends both on the time-of-flight T and

[a] e-mail: lukich@nfi.kiae.ru
[b] e-mail: yakovlev@theor.mephi.msk.ru
[c] e-mail: vitpal@mail.ru

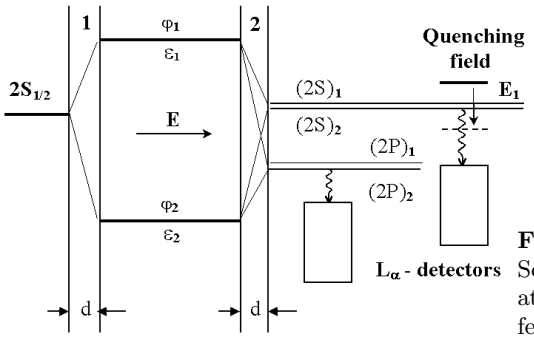

Fig. 1. Scheme of the atomic interferometer.

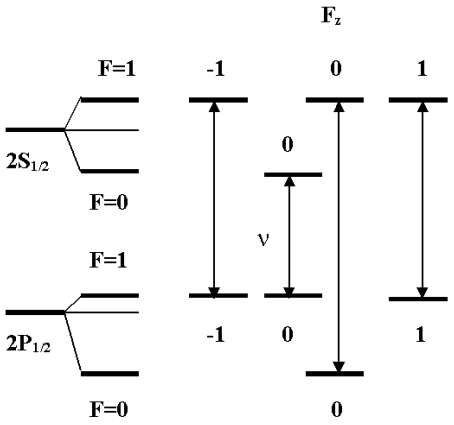

Fig. 2. The hyperfine structure of $2S_{1/2}$ and $2P_{1/2}$ levels of a hydrogen atom.

on the frequency $(\varepsilon_1 - \varepsilon_2)/\hbar$ of the transition between terms ε_1 and ε_2. The latter, in turn, is determined by the field strength E. As a result, the monotonic change in the field strength will be accompanied by periodic counterphase oscillations in the flux intensity of 2S and 2P atoms, caused by the interference of the $(2S)_1-(2S)_2$ contribution and, similarly, of the $(2P)_1-(2P)_2$ contribution. The same picture will be observed at gradual change of time-of-flight, *i.e.* the distance between boundaries 1 and 2.

The interferometer based on the above principle is similar to a two-beam optical interferometer in which an individual photon interferes with itself. Two "channels", φ_1 and φ_2, appear here due to the electric field playing the role of the semi-transparent mirror that splits the evolutionary "paths". It mixes the states with opposite parity, so the initial 2S state receives a coherent addition of the 2P state.

The interference pattern of the short-living $2P_{1/2}$-state ($\tau = 1.59 \times 10^{-9}$ s) is observed by measuring the flux of L_α-quanta, which result from one-photon transitions to $1S_{1/2}$-state. To observe the interference of the metastable $2S_{1/2}$-state, the quenching field E_1 is used.

Note that for comparatively weak fields (when the Stark shift is of the order of the Lamb shift), the analysis can be simplified by considering only the two-level system $2S_{1/2}-2P_{1/2}$ and by introducing small corrections to account for the effect of the $2P_{3/2}$-level. The hyperfine structure of the $2S_{1/2}$ and $2P_{1/2}$-states is shown in Figure 2. All experiments described below were performed with a

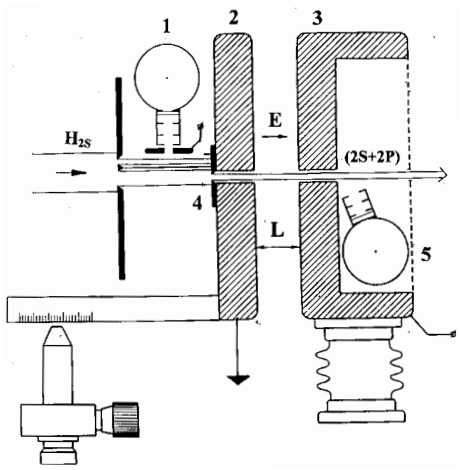

Fig. 3. Scheme of the two-electrode interferometer with a longitudinal field: 1 – detector of the 2S-monitor; 2 and 3 – flat electrodes with slits for passing the beam; 4 – collimator slit; 5 – L_α detector.

beam from which the $2S_{1/2}$-component with the total angular momentum $F = 1$ was removed by a high-frequency field. In this case the observed interference pattern corresponds to the transition between the states $|1\rangle \equiv |2S_{1/2}, F = 0, F_z = 0\rangle$ and $|2\rangle \equiv |2P_{1/2}, F = 1, F_z = 0\rangle$ with the frequency $\nu = 909.9$ MHz.

Figure 3 shows the scheme of the simplest atomic interferometer consisting of two plane electrodes producing the field E and separated by a variable distance L. On the electrodes, there are two slits for the beam passage. The width of the slits meets the condition of the non-adiabatic change of the field E at the boundaries.

3 The asymmetry of the 2P-state yield in the atomic interferometer

In the ideal two-electrode interferometer, the yield of the 2P-atoms does not depend on the direction of the field E, provided that the atoms enter this field in the pure 2S-state. This is due to the electric field mixing the states with the opposite parity. Therefore if an atom entering the field is in a state with certain parity (2S or 2P), its output amplitude in the same state is an even function of the field, while the output amplitude with the opposite parity is an odd function, correspondingly. Hence the output probability of any state is an even function of the field and thus is independent of the sign of E[1].

[1] We note for completeness that with account of relativistic effects, the dependence of the decay probability of the 2S-state on the direction of the external electric field E appears due to the interference of $E1$ and $M1$ decay channels. The interference term depends linearly on E and yields an asymmetric correction to the radiation intensity, which changes the sign with changing the field direction. This effect emerges in very weak fields and was discussed, in particularly, in connection with the problem of parity violation in hydrogen atoms [20]. The maximum value of the asymmetry parameter

In our experiments, atoms entering the interferometer field were in the pure 2S-state. Nevertheless, as a rule the yield of 2P-atoms was found to be different for the opposite signs of the field: the interference curves do not coincide after the field reversal. The question arises as to what is the reason for such a discrepancy?

The most simple, and apparently natural, explanation to the discovered effect is the assumption that it is due to the action of electric fields δE generated by charges appearing for some reason on the surface of the metallic slits. The effect of such fields depends on their location in the system of the two-electrode interferometer. If the field δE is generated by a charge on the surface of the normal to the beam electrodes that form the field E, the effective field affecting atoms in the interferometer will be $E_{\text{eff}} = E + \delta E$. Since the output probability is an even function of E_{eff}, the difference in the interference curves $I_{2\text{P}}(\pm E)$ corresponding to two signs of the field E reduces to the simple of the shift by $2\delta E$. A different physical picture emerges if the field δE (or some other perturbation) arises inside the slits in the electrodes. In this case, for example, 2S-atoms flying through the slit in the first electrode, will be in a superposition of the $2\text{S} - 2\text{P}$-states by the moment of interaction with the field E. An uncertain parity of the superposition input state results in the asymmetry of the 2P-state output probability $I_{2\text{P}}$ with respect to the sign of E.

To understand the structure and possible location of such arbitrary arising fields we studied the interference curves $I_{2\text{P}}(\pm E)$ for different atomic energies ranged from 17 to 26 keV. For the inter-electrode space 0.5 cm the time-of-flight was about 2.5×10^{-9} s and subjected to variation $\pm 12\%$.

At low energies a significant discrepancy of the curves $I_{2P}(\pm E)$ was observed (Fig. 4a). In contrast, at energies near 26 keV it proved possible to find the energy (*i.e.* the time-of-flight in the field E) such, that the curves for the opposite signs of the field become indistinguishable within the measurement accuracy (Fig. 4b). Note also that the interference curves shown in Figure 4a can not be matched by simple shifting of the variable E.

The above results lead to the following conclusions:

1. the electric field δE caused by charges on the surface of normal-to-beam electrodes, even if such charges exist, is negligibly small and can not change the yield of 2P-atoms with the field E reversal;

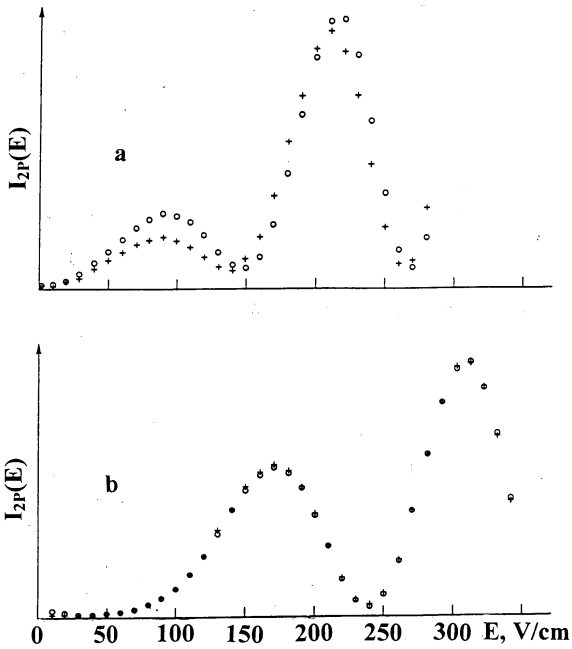

Fig. 4. Interference curves for the energies 17 keV (a) and 26 keV (b). The line with (∘) symbols corresponds to the field which is in the same direction as the velocity of atoms; (+) line – the field has an opposite direction.

2. at the same time, the fact that in the experiment the time-of-flight can be found such that the interference curves coincide for the opposite directions of the field E, evidences that the output asymmetry of 2P-atoms is due to the influence of slits in the interferometer electrodes. For a certain value of the time-of-flight, these effects compensate each other. In other words, an excited hydrogen atom flying near the metal wall of the slit, somehow interacts with it, that results in the coherent mixing of the 2S and 2P states.

The surprising is not the very fact of such an interaction, but huge distances at which it acts. As was shown in experiments [16,19], the formation of 2S–2P-superposition was registered, within the detector's sensitivity limits, up to distances of the order of 0.7 mm between the atom's trajectory and the metal surface.

This interaction is clearly visible in the simple experiment schematically shown in Figure 5. A beam consisting of a mixture of 1S and 2S hydrogen atoms with an energy of about 22 keV passes through a system comprising the quenching field 1 (to remove 2S-atoms from the beam), the collimator 2 (to give the beam a band-like shape with a cross-section of 0.05×2 mm), the slit 3 with a width of 0.3 mm, the slit 4 (the same as the slit 3), and the detector 5 of L_α-quanta rigidly connected to the slit 4. The space between the slits 3 and 4 can vary from 0.2 to 15 mm. The slits are made of plate bronze with 0.8 mm in thickness and are galvanically coated with a ~ 5 μm gold layer. The slits are carefully grounded.

The results of the experiment are shown in Figure 6.

$B = (I_+ - I_-)/(I_+ + I_-)$, where I_+- stand for the radiation intensities for the opposite directions of the field E, is attained for equal probabilitites of the magneto-dipole decay of the 2S-state and of the dipole transition $2\text{P}-1\text{S}$ induced by the electric field. For $E = 3 \times 10^{-5}$ V/cm this value is 5%, and for spin-polarized states can be close to unity [8]. In the interesting for us situation, when the field is not that weak, the magneto-dipole transition probability is much smaller than that of the induced dipole transition, and the parameter B is estimated to be $Z^8 \times 2.8 \times 10^{-6}$ [8,9], where Z is the charge of the nucleus. So for $E \sim 1$ V/cm the asymmetry parameter is very small, of the order of 3 ppm.

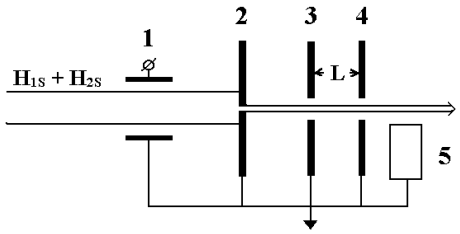

Fig. 5. Scheme of the experiment without an external field (explanations in the text).

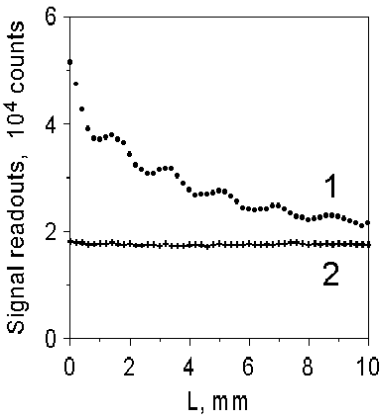

Fig. 6. Results of the experiment without an external field (explanations in the text).

If the quenching field is turned on, *i.e.* in the case where only 1S-atoms pass trough the system, a background is registered (the curve 2) which is mainly due to a noticeable amount of H-atoms appearing at different excitation states under the action of electrons kicked out by the beam of the frontal wall of the collimator 2. Cascade transitions to the 1S-state in such atoms yield a L_α-radiation whose intensity decreases with the distance from the collimator and, starting from a distance of about 20 mm, remains practically constant within the interval $\delta L \sim 10$ mm (that is why the space between the collimator 2 and the slit 3 was chosen to be at least 20 mm). It is necessary to note that the constant value of the background along the entire length δL (which also includes the component due to the atomic collisions with the rest gas molecules) evidences for the beam flying through the 0.3 mm slit 3 not touching its walls. This implies that the beam halo has a small size and does not affect the observed phenomenon [16].

If the quenching field is turned off, 2S-atoms pass through the system, and distinctive oscillations of the flux of 2P-atoms are visible (the curve 1), *i.e.* the interference of this state appears. The oscillation amplitude gradually decreases and becomes unmeasurable at $L > 20$ mm. The registered asymptotically smooth curve, locates somewhat above the curve 2.

All the experimental results can be phenomenologically described as follows. The effect of each of the slits 3 and 4 on an atom represents a small perturbation which results in the $|2S\rangle$ state transforming into a superposition $|2S\rangle + b|2P\rangle$ with small mixing amplitude b. Then the resulting output probability $I_{2P}(L)$ of 2P-atoms has the form [16]

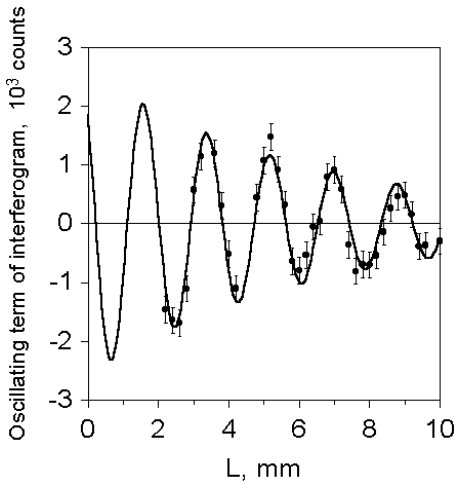

Fig. 7. Interference of the 2P-state. The solid line is a fitting of the third term from equation (1) to the experimental points.

$$I_{2P} = |b_1|^2 \exp\left(-\frac{\gamma L}{\upsilon}\right) + |b_2|^2 + 2|b_1 b_2| \exp\left(-\frac{\gamma L}{2\upsilon}\right) \cos\left(-\frac{2\pi\nu L}{\upsilon} + \varphi\right). \quad (1)$$

Here $b_{1,2}$ are small mixing amplitudes of 2S and 2P states by the slits 3 and 4, υ is the atomic velocity, $\gamma = 0.6265 \times 10^8$ s^{-1}, $\nu = 909.8394$ MHz is the Lamb shift. The L-independent phase φ is determined by the action of both slits 3 and 4. For close parameters of these slits it is naturally to assume that the amplitudes $|b_1|$ and $|b_2|$ do not differ significantly. Therefore for not too large L, *i.e.* when $L < \upsilon/\gamma \cong 2.9$ mm, all terms in equation (1) are of the same order of magnitude.

Equation (1) implies that the dependence $I_{2P}(L)$ is a superposition of two curves. The first two terms that include the decay exponent of the 2P-state and the constant $|b_2|^2$ describe the mean line. The third term is an oscillating function of L and describes the interference curve of interest here. The latter can be obtained by subtracting the mean curve from the total curve (Fig. 7).

The scale of the effect observed can be conveniently characterized by parameter $2|b_2/b_1|$, *i.e.* by the ratio of the amplitude $2|b_1 b_2|$ of the interference term to the coefficient $|b_1|^2 = I_{2P}(0)$.

The equation above shows that the space oscillation period of the curve is $\Lambda_L = \upsilon/\nu$. For $\upsilon = 2.2 \times 10^8$ cm/s, the theoretical value Λ_L is 0.22 cm, which is in a good agreement with the experimental one. Note that Λ_L does not contain any characteristics of atom-metal surface interaction. All parameters of such an interaction enter the coefficients b_1, b_2 and the phase φ. From this point of view, equation (1) should be considered as a phenomenological parameterization of the interference effect which is adequate to experimental situation. Moreover, we necessarily

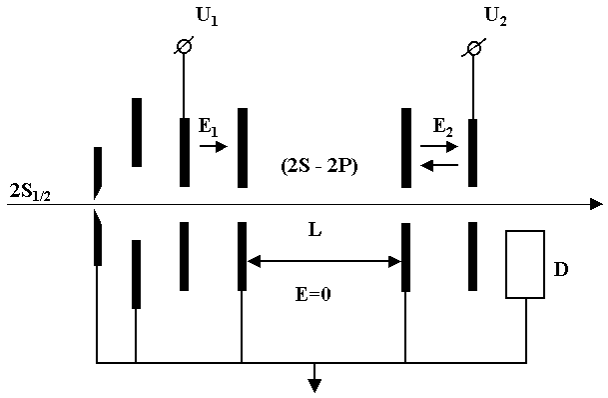

Fig. 8. Scheme of a double interferometer (explanations in the text).

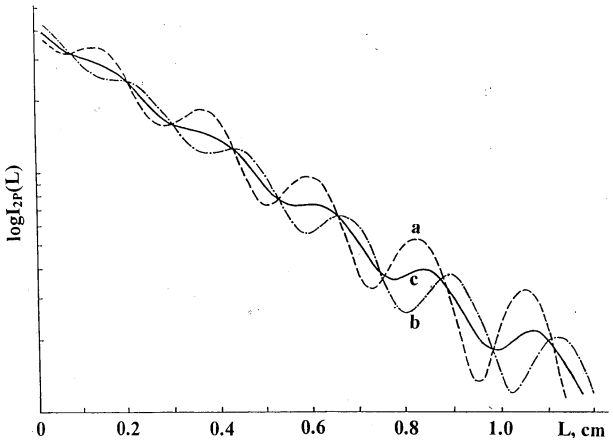

Fig. 9. Results of experiments with the double interferometer, shown in Figure 8.

arrive at the following interpretation of the phenomenon: in the slit 3, an interaction of a 2S-atom with metallic walls results in a coherent mixing of 2S and 2P states, *i.e.* in the formation of 2S−2P superposition. In the slit 4, a similar interaction leads to an additional mixing of these states, so periodical oscillations in the flux of 2P-atoms appear when changing the distance L, *i.e.* the interference of this state is observed.

Thus, the key question is what is the mechanism for interaction of atoms with metal surfaces of the slit that leads to the coherent mixing of 2S and 2P states.

4 The "double" atomic interferometer

As was mentioned above, the most simple explanation to the effect discovered is the assumption that it is due to the action of electric fields generated by charges that appear for some reasons on the surface of metallic walls of the slits. Doubts in this explanation arose mainly due to a steady reproducibility of the experimental results, which would be impossible for the chaotic character of the randomly arising charges. Nevertheless, the assumption on the presence of the electric charges on the metal surface could not be entirely rejected, since the total amount of data obtained at the first stage of the experiment could be explained by the effect of electric fields localized in the interferometer slits.

In experiments designed to study a possible influence of such fields, the interferometer shown in Figure 8 was used. It comprised systems I and II separated by a distance L. The detector D rigidly connected with the system II measures the flux of 2P-atoms. The superposition of 2S−2P states is produced by the electric field E_1 aligned with the atomic velocity vector (the longitudinal filed). In the system II atoms are influenced by both the electric field E_2 and perturbation due to their interaction with metallic walls of the slits, which phenomenologically can be related with the "electric" field E_3. Thus, in the system II, the effective field $E_{\text{eff}} = E_3 \pm E_2$ acts on atoms.

Such a "double" interferometer allows us to do a gauge experiment, *i.e.* to compare the actions of the fields E_3 and E_2. To this aim, three measurements of the flux of 2P-atoms were performed for each value of L: at $E_2 = \pm 15$ V/cm and for shortened and grounded electrodes of system II, *i.e.* for the case where the field E_2 is zero.

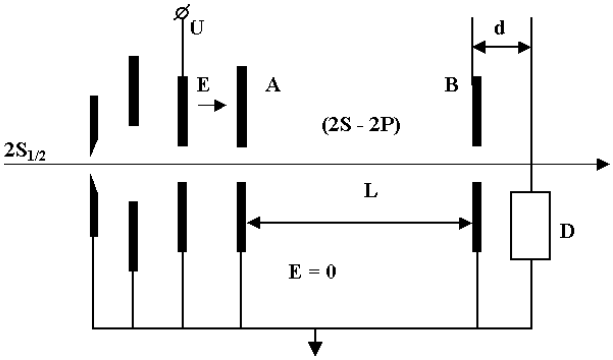

Fig. 10. Variant design of a double interferometer.

The results of the experiment with $E_1 = 57$ V/cm are shown in Figure 9. As expected, the flux oscillations of 2P-atoms produced by E_2 fields with opposite signs occur in counter-phase (curves a and b). At the same time, the distinct interference picture is observed in the absence of the field E_2 (curve c), which can be explained only by interaction between atoms and metal slits. The scale of the effect, *i.e.* the oscillation amplitude, corresponds to the action of the field E_3 with a strength of about 10–12 V/cm. The curve c is shifted with respect to the curves a and b, which can be explained by different configurations of the fields E_2 and E_3. Nevertheless, Figure 10 shows that the field E_3 is apparently aligned with the direction of the velocity of atoms.

One of the tests in a series of measurements performed with the interferometer shown in Figure 10 consisted in observing the deexcitation of the 2P-component of the 2S−2P superposition. In that case the system II was set as a 3 mm slit B cut in a plate 0.8 mm in thickness. Within the device's sensitivity, such a wide slit was not found to have any effect on flying-through atoms (recall

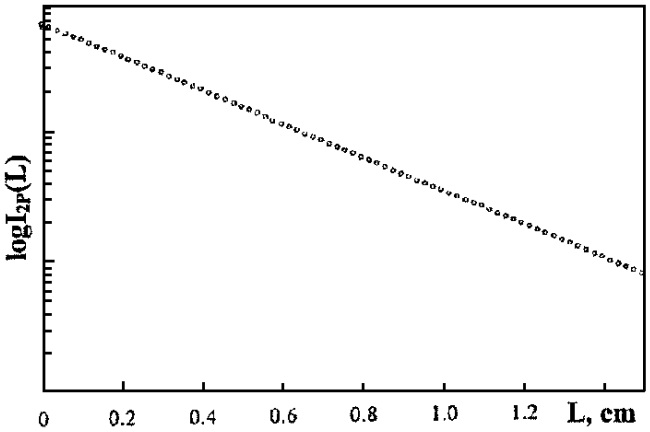

Fig. 11. Decay curve of the 2P-state.

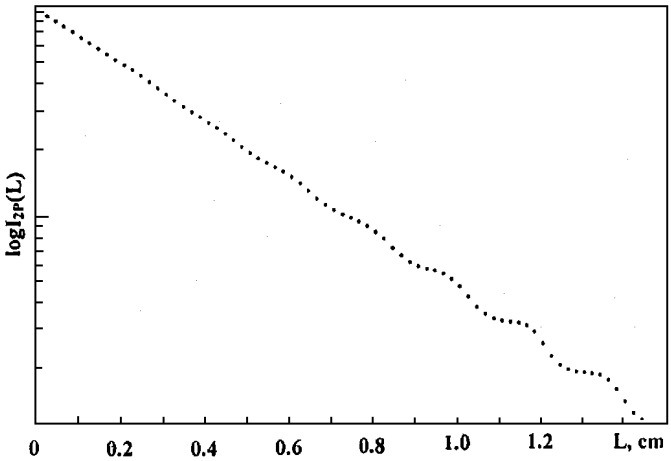

Fig. 12. The $I_{2P}(L)$-dependence for the 0.4 mm slit.

that the beam has a shape of a band with cross-section 0.05×2 mm).

With a constant longitudinal field $E_1 = 380$ V/cm in the first system the intensity of 2P-atoms flux was measured as a function of the distance $l = L + d$ between the output (grounded) electrode A of the system I and the detector D. This dependence written in semi-logarithmic scale

$$\ln I_{2P} = \text{const} - \frac{\gamma l}{v} \tag{2}$$

represents a straight line (Fig. 11), whose slope allows, by the way, to determine the atomic velocity provided the life-time of a 2P-atom is known, and *vice versa*.

The data obtained evidence for the absence of the electric field along the total length l, *i.e.* both between plates A and B and along the interval d. Indeed, if such a distance-L-depending field were present, the decay of the 2S-component of the superposition would also take place, which would distort the shape of function $I_{2P}(l)$.

In the subsequent version of the experiment, the slits with width varying from 2.5 to 0.2 mm were used. In these cases the curve of the dependence $\ln I_{2P}(L)$ remained practically unchanged, *i.e.* represented a straight line up to the slit width of about 1.4 mm. For narrower slits, 2P-atom flux intensity oscillations appeared with the amplitude increasing with the slit width decreasing. The curve obtained for the 0.4 mm slit (Fig. 12) demonstrates a distinctive interference pattern of the 2P-state and is described by equation (1), which indicates the absence of the electric field along the distance L.

Figure 13 shows how the scale of the effect depends on the slit width, *i.e.* on the distance between the atom's trajectory and the metal surface.

Thus, the results of the above experiments are as follows:

1. the electric field in the space between grounded plates A and B (*i.e.* along the length L), as well as behind the plate B (*i.e.* along the length d) is not detected;
2. at distances $\leq$0.7 mm between the slit surface and a flying atom, a perturbative action of the slits emerges, which leads to a coherent mixing of the 2S and 2P states.

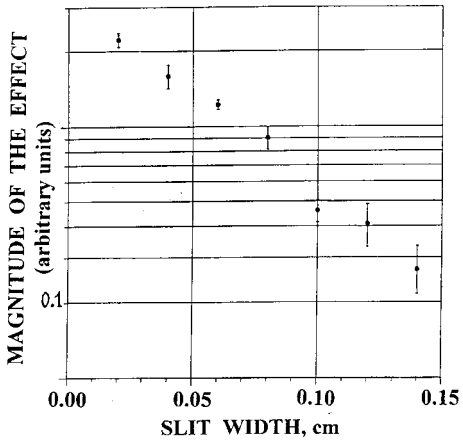

Fig. 13. The scale of the effect as a function of the slit width.

These results are in full agreement with data obtained using the two-electrode interferometer (Figs. 4a and 4b).

5 The interference of 2S and 2P atomic states for different orientations of electric fields

In the interferometer shown in Figure 8, the system II can consist either of two electrodes producing the field E_2 or of a single slit of different configuration, producing the field E_3. Let us first consider the conditions for the interference of 2S- and 2P-states to appear, when in systems I and II electric fields E_1 and E_2, arbitrarily oriented with respect to each other, act on an atom. Clearly, it is sufficient to consider two cases when these fields are parallel or orthogonal each other

5.1 The case of parallel fields

We choose the axis z (the quantization axis) along the direction of the parallel fields E_1 and E_2. This axis can be

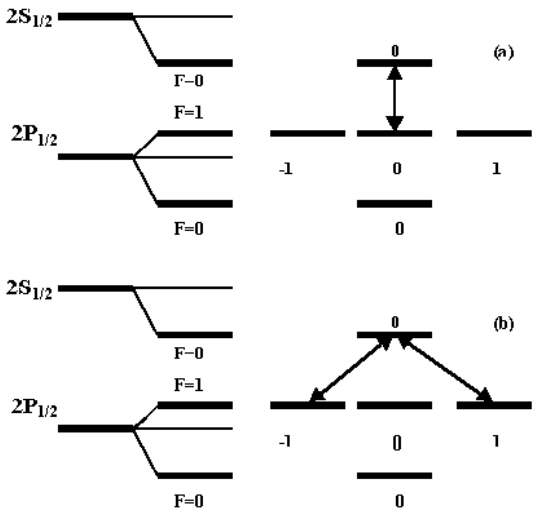

Fig. 14. Mixing of states 2S–2P, caused by longitudinal (a) and transverse (b) fields.

arbitrarily directed with respect to the velocity v. However, two cases are of practical interest: either the axis z coincides with or is normal to the velocity v. Figure 14a shows the scheme of the superfine structure of $2S_{1/2}$ and $2P_{1/2}$ states of hydrogen atom with the $2S_{1/2}$-state component with the total moment $F = 1$ removed. The arrow on the scheme connects the states with non-zero matrix elements of the dipole momentum operator d_z. Thus, in each of the systems I and II, the mixing of one and the same pair of the states $|1\rangle \equiv |2S_{1/2}, F = 0, F_z = 0\rangle$ and $|2\rangle \equiv |2P_{1/2}, F = 1, F_z = 0\rangle$ occurs, since at the system I input atoms were in the state $|1\rangle$.

After passing through the electric field E_1, atoms are in the superposition of the states $|1\rangle$ and $|2\rangle$. As there are no perturbations between systems I and II, the superposition coefficients freely evolve here. At last, in the system II, the field E_2 causes again a coherent mixing of the states $|1\rangle$ and $|2\rangle$. Therefore each of the coefficients in the resulting superposition is the sum of two phase-shifted terms, which results in the interference. The interference effect is described by oscillating terms of the term

$$\exp\left(-\frac{\gamma L}{2v}\right)\cos\left(\frac{2\pi\nu L}{v}+\varphi\right) \qquad (3)$$

in the populations of both 2S and 2P-states. We emphasize that we deal with a general principle: the interference appears when the resulting amplitude of a quantum state contains coherent contributions from the states which evolved along different "paths".

5.2 The case of orthogonal fields

Now the fields E_1 and E_2 are orthogonal. Let the direction of the field E_1 be the quantization axis z, the direction of the field E_2 be the axis x. In the system I, as in the previous case, the mixing of the states with non-zero matrix elements of the operator d_z occurs. With account of the previous initial condition, the system I thus composes a superposition of the same states $|1\rangle$ and $|2\rangle$, which after the free evolution over the distance L enters the second system.

The states with non-zero matrix elements of the operator d_x are mixed in the system II. This pairs of states are connected by arrows in Figure 14b, which mark transitions with account of the initial states of atoms entering system II. Thus in this system the field E_2 (transversal with respect to the field E_1) does not produce an additional coherent mixing of $|1\rangle$ and $|2\rangle$ and the interference effect is absent. The transversal field only change the L_α-background due to transitions shown in Figure 14b, but does not result in interference.

Based on the analysis, in one of the experiments a slit with a special shape was used as system II (slit B, Fig. 10), in which the electric field caused by some potential difference between its walls could be only *transversal* and the observed effect could appear only due to longitudinal components formed by the field warping. The 0.3 mm slit was formed by two sharp *strictly coplanar* blades made of hard bronze coated with a ~ 5 μm gold layer. In this case, a distinctive interference pattern emerges which can be only due to a *longitudinal* field whose strength must be of the order of 12 V/cm. If the detected effect was due to longitudinal components of the field related to the transversal field warping, the strength of the latter should be ~ 400 V/cm, which corresponds to an inter-blade potential difference of 12 V. Clearly, such a potential difference would completely distort the interference pattern due to the fields of uncertain configuration appearing between blades and grounded parts of the interferometer.

It seems unlikely that a stable potential difference of 12 V with one and the same polarity can arbitrarily arise between two grounded golden blades. Nevertheless, the interference is steadily detected from test to test with both golden coatings of different thickness and the slits entirely made of plates of gold, silver, and palladium, whose surface is free from "spot-like" structures characteristic to galvanic metal coatings.

As an antipode to the "knife-like" slit, the slit shown in Figure 15 was used (the width of the slit was 0.3 mm with a length of 6 mm). Again, quite distinctive interference pattern was observed. It is essential that interference curves obtained in these experiments are described by equation (1), which evidences for the lack of distortions of the dependence $I_{2P}(L)$ that could appear if a longitudinal field would exist over the distance L. This implies that the interference is caused by a perturbation due to atomic interactions with the slit's walls. It should be stressed that the perturbing factor can not be an electric field, especially *longitudinal*, since such a field can not exist in a cavity inside metal.

Finally, the last possible location of the longitudinal electric field producing the interference can be the *rear* wall of the slit, on which some charges appeared for some reasons (they are not present on the *front* wall). Such a field can be detected by observing the decay of 2P-component on the interval between the rear wall of the

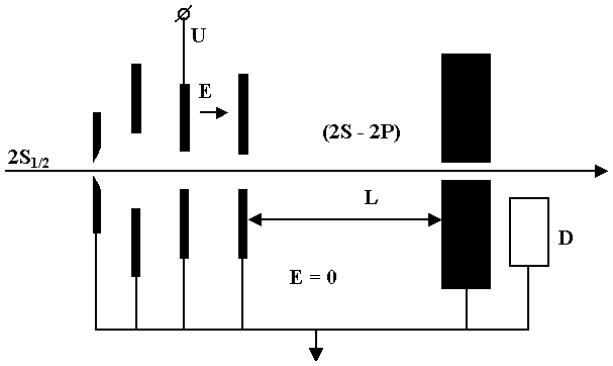

Fig. 15. Experiment with a long slit in absence of an external field.

slot and the detector. Such a measurement is quite similar to repeatedly made experiments on observing the 2P-state decay (for example, to the test shown in Fig. 11). These experiment implied that there were no electric fields distorting theoretical relation (2) along the beam trajectory.

6 Conclusion

What logic was behind the consequent experiments aimed understand physical mechanism responsible for a large coherent mixing of the 2S and 2P states resulting in a well-pronounced interference pattern?

First of all, it was quite natural to assume that the observed effect could be produced by an electric field E created by charges arising on the metal surface. All attempts to get rid of such a field (we even nicknamed it the "demon field") by using of various cleansing methods of the metal surfaces technologies of the processing etc., have ended in failure. Really, it was necessary to admit, that the origination of the field E is conditioned by several, beforehand unknown factors of different nature. Their detection seemed to be a hopeless problem and therefore an other approach was adopted: assuming the existence in interferometer system of a random electric field, strong enough ($\sim$10 V/cm) and directed along the atom velocity, we attempted to find out its presence in a series of specially designed experiments. The result was negative.

Therefore, the consistent conclusion which follows out from the experiments considered here, is that the discovered effect is due to unknown long-range interaction between an excited hydrogen atom and a metal surface.

But what is the nature of such an interaction?

Presently, a lot of theoretical and experimental studies of interaction of hydrogen atoms with metallic surfaces are known.

For microscopic distances ($R \sim 1{-}10$ μm) between a hydrogen atom and a metal surface, three main effects are usually considered that describe long-range van der Waals and Kasimir forces and the resonance radiation shift [21–24]. According to Lifshits's theory [25], at zero temperature the potential energy of a neutral atom at a distance R from a conducting surface is determined by

$$V_L(R) = -k_L/R^3, \tag{4}$$

where

$$k_L = \frac{\hbar}{4\pi}\int_0^\infty \mathrm{d}u\alpha(\mathrm{i}u)\frac{\beta(\mathrm{i}u)-1}{\alpha(\mathrm{i}u)+1} \times \left(1+\frac{Ru}{c}\right)^2 \exp\left(-\frac{2Ru}{c}\right). \tag{5}$$

This equation takes into account the retardation effects; $\alpha(\mathrm{i}u)$ and $\beta(\mathrm{i}u)$ are the atomic polarizability and the metal's dielectric function, respectively, c is velocity of light. In the limit of small distances the parameter k_L is a constant value and equation (4) describes the classical van der Waals potential. In this limit, the atom-surface interaction can be interpreted as a fluctuating interaction of an atomic dipole moment with its "mirror" reflection in the metal. In the limit of large distances the parameter k_L

$$k_L = \frac{5\hbar c\alpha(0)}{16\pi R} \tag{6}$$

is the so-called Kasimir parameter. In this limiting case the shift of the hydrogen atom level can be treated as the Stark shift caused by the change in boundary conditions (due to the presence of a conducting medium) for vacuum fluctuations of the field.

In hydrogen atoms, the van der Waals interaction leads only to a scalar shift of S-states [26,27]. For example, for 1 μm distance the shift of the 2S-level is -2.3 kHz. For the 2P-level the van der Waals potential leads to interaction with the 2S-state, and the Kasimir potential determines interaction with other ns-states. The total shift of the 2P-level caused by these interactions is -0.8 kHz. The resonance radiation shift at large distances is described by the oscillating function

$$\delta_{2\mathrm{P}} = \frac{\hbar}{2}\Gamma_{2\mathrm{P}}\frac{\cos(2kR)}{2kR}\,. \tag{7}$$

Here the wave vector k corresponds to 2P$-$1S transition. For 1 μm distance the oscillation amplitude is 500 kHz and is numerically dominant factor determining the shift of np-levels at large distances from a conducting surface. It should be noted that the above estimates [26,27] quite appreciably differ from analog results obtained in [28,29] that used QED-approach to calculate the Lamb shift under given boundary conditions.

Of other publications devoted to this problem, references [30–35] should be noted, in which spectroscopic constants for hydrogen were calculated using imaginary charge approximation. It was shown, in particular, in [30] that in the excited state of hydrogen with a constant dipole moment, a linear Stark effect is present, which is similar to the conventional Stark effect in a homogeneous electric field. In [35], energy levels of hydrogen were calculated as a function of the atom-surface distance using numerical solution of the Schrödinger equation. The blackbody radiation effect on the life-time of the 2S-state of hydrogen is considered in [36].

To summarize, the above theoretical estimates give a negligible small value of the atom-metal-surface interaction when we deal with distances of the order of 200−700 μm. Indeed, the long-range interaction observed in our experiments exceeds the well-known results at least by two-three orders of magnitude. It means that under experimental conditions the atom-metal-surface interaction exhibits some new features which are beyond the standard mechanisms.

Recently two quite different interpretations of the effect were proposed in references [37–39]. According to the works [37,38] the 2S atom and individual electrons located in a thin surface layer of metal form a huge number of EPR-pairs given rise to a coherent admixture of the 2P state. In contrast to the mechanism [37,38] appealing to "physical nonlocality", the interpretation given in reference [39] is based, let us say, on pure "physical locality". Without going into details we only mention that the external state of of the hydrogen atom in the beam is treated as a wave packet. Small parts of the center-of-mass wave function, *i.e.* tails of halo, can penetrate the metal surface up to a high field area that results, according to [39], in a coherent mixing of the 2S and 2P states.

We note that certain doubts [40] are cast on the principal for the approach [37,38] point concerning the coherence in the system "atom + conductive electrons". Nevertheless the proposed interpretation is worth a careful experimental checking which is carrying out at the present time.

Recent experiments [16] showed that the scale of interaction strongly depends on the microcrystalline structure of the metal surface. In these experiments we used the slits formed by massive plates of gold-silver alloy and pure palladium. During the experiment the microstructure of the plates was considerable varied-namely, the plates were initially highly cold-hardened samples and later on they were annealed at the recrystallization temperature. In other words, we performed measurements with either fine-grained or coarse-grained metal surfaces. It was found that for both metals the mixing amplitude displayed a severalfold, by the factor of 5–7, increasing after annealing. These important results can serve in benefit of a significant role played by conductive electrons from the surface layer.

Now we take into account this fact and recall that the effect itself looks like an interaction with some "effective electric field" $\mathbf{E}_*$ directed along the atomic velocity $\boldsymbol{v}$. It means that the vector $\mathbf{E}_* \sim \boldsymbol{v}$ is built up from the only vector $\boldsymbol{v}$ existing in the system, while the coefficient may depend on characteristics of quasi-free electrons (charge e, mass m) and on the distance R between the atom and the metal surface. Using heuristic arguments, such as the proper dimension and maximal simplicity of the result, we arrive at

$$E_* = \eta \frac{em}{\hbar} \frac{v}{R} \,. \tag{8}$$

Here the parameter η characterizes the fraction of free charge carries and may be estimated as $\eta \sim \tilde{T}/\varepsilon_{\rm F}$, where $\tilde{T}$ and $\varepsilon_{\rm F}$ denote the temperature and the Fermi energy of an electron gas. Then equation (8) qualitatively coincides with the results [37,38]. If $v \sim 2 \times 10^8$ cm/s, $R \sim 10^{-2}$ cm and $\eta \sim 10^{-2}$ cm, equation (8) gives $E_* \sim 10$ V/cm and therefore reasonably corresponds to experimental data. We are not disposed to over-rate the significance of the empirical relation (8). Nevertheless the temperature and velocity dependence of the "effective electric field" $\mathbf{E}_*$ given by equation (8) is worth a further experimental checking.

Physical mechanism responsible for a large-scale coherent mixing amplitude is the challenge of the interference experiments with metastable hydrogen atoms. Though the present results are still of qualitative character, the observed strong dependence of the mixing amplitude on the crystal structure of metal samples allows us to be more confident about an important role of conductive electrons from a thin surface layer of metal. Further quantitative experiments, using high sensitivity interference method, aim to identify physical parameters of surface microstructures which may be responsible for a long-range atom-surface interaction.

The authors are grateful to Yu.A. Kucheryaev and G. von Oppen for help and fruitful discussions and to M.S. Aksent'eva for valuable advices. We gratefully acknowledge interesting discussions with S.T. Belyaev on details of his unpublished paper. The work was supported by the Russian MINPROMNAUKA (grant 01-53), by the Russian Foundation for Basic Research (grants RFBR 01-02-16516, 01-02-17643 and 01-02-97013R) and by the Volkswagen Stiftung (Federal Republic of Germany, grant I/68770).

References

1. F. Biraben, T.W. Hänsch, M. Fischer, M. Niering, R. Holzwarth, J. Reichert, Th. Udem, M. Weitz, B. de Beauvoir, C. Schwob, L. Jozefowski, L. Hilico, F. Nez, L. Julien, O. Acef, J.-J. Zondy, A. Clairon, in *The Hydrogen Atom. Precision Physics of Simple Atomic Systems*, edited by S.G. Karshenboim, F.S. Pavone, F. Bassani, M. Inguscio, T.W. Hänsch (Springer-Verlag, Berlin, 2001), p. 17; E.G. Myers, *ibid.*, p. 179
2. Yu.L. Sokolov, V.P. Yakovlev, V.G. Pal'chikov, D.N. Lin, Nuovo Cimento D **14**, 183 (1992)
3. Yu.L. Sokolov, V.P. Yakovlev, V.G. Pal'chikov, Laser Phys. **3**, 635 (1993)
4. Yu.L. Sokolov, V.P. Yakovlev, V.G. Pal'chikov, Phys. Scripta **49**, 86 (1994)
5. M. Goppert-Mayer, Ann. Phys. (Lpg) **9**, 273 (1931)
6. G.W.F. Drake, Phys. Rev. A **34**, 2871 (1986)
7. W.E. Lamb Jr, Phys. Rev. **85**, 259 (1952)
8. G.W.F. Drake, Phys. Rev. Lett. **40**, 1705 (1978)
9. P.J. Mohr, Phys. Rev. Lett. **40**, 854 (1978)
10. M. Hillery, P.J. Mohr, Phys. Rev. A **21**, 24 (1980)
11. J.P. Levy, Phys. Rev. A **29**, 3189 (1984)
12. H.K. Holt, Phys. Rev. A **28**, 1157 (1983)
13. A. van Wijngaarden, F. Holuj, G.W.F. Drake, Can. J. Phys. **76**, 95 (1998)
14. A. van Wijngaarden, J. Kwela, G.W.F. Drake, Phys. Rev. A **43**, 3325 (1991)

15. V.G. Pal'chikov, Yu.L. Sokolov,V.P. Yakovlev, in *The Hydrogen Atom. Precision Physics of Simple Atomic Systems*, edited by S.G. Karshenboim, F.S. Pavone, F. Bassani, M. Inguscio, T.W. Hänsch (Springer-Verlag, Berlin, 2001), p. 352
16. Yu.L. Sokolov, Usp. Fiz. Nauk. **169**, 559 (1999) [Phys. Usp. **42**, 481 (1999)]
17. Yu.L. Sokolov, V.P. Yakovlev, Zh. Eksp. Teor. Fiz. **83**, 15 (1982) [JETP **56**, 7 (1982)]
18. V.G. Pal'chikov, Yu.L. Sokolov, V.P. Yakovlev, Metrologia **21**, 99 (1985)
19. V.G. Pal'chikov, V.P. Yakovlev, Yu.L. Sokolov, Phys. Scripta **55**, 33 (1997)
20. E.A. Hinds, in *The Hydrogen Atom*, edited by F. Bassani, M. Inguscio, T.W. Hänsch (Springer-Verlag, Berlin, 1989), p. 268
21. S. Haroche, J.M. Raimond, in *Advances in Atomic and Molecular Physics*, edited by D. Bates, B. Bederson (Academic, New-York, 1985), Vol. 20, p. 347
22. D. Meschede, W. Jhe, E.A. Hinds, Phys. Rev. A **41**, 1587 (1990)
23. G. Barton, J. Phys. B **7**, 2134 (1974)
24. J.M. Wylie, J.E. Sipe, Phys. Rev. A **30**, 1185 (1984); *ibid.* A **32**, 2030 (1985)
25. E.M. Lifshitz, Zh. Eksp. Teor. Fiz. **29**, 94 (1955) [Sov. Phys.-JETP **2**, 72 (1956)]
26. E.A. Hinds, in *Advances in Atomic and Molecular Physics*, edited by D. Bates, B. Bederson (Academic, New-York, 1990), Vol. 87, p. 235
27. E.A. Hinds, V. Sandoghdar, Phys. Rev. A **43**, 398 (1991)
28. Il-Tong Cheon, Phys. Rev. A **37**, 2785 (1988)
29. Il-Tong Cheon, S.D. Oh, J. Phys. Soc. Jpn **58**, 1581 (1989)
30. A.V. Chaplick, Zh. Eksp. Teor. Fiz. **54**, 332 (1968) [Sov. Phys.-JETP **29**, 372 (1968)]
31. P. Nordlander, J.C. Tully, Phys. Rev. Lett. **61**, 990 (1988)
32. P. Nordlander, J.C. Tully, Phys. Rev. B **42**, 5564 (1990)
33. A.G. Borisov, D. Teillet-Billy, J.P. Cauyacq, Nucl. Instrum. Meth. B **78**, 49 (1993)
34. S.A. Deutscher, X. Yang, J. Burgdörfer, Phys. Rev. A **55**, 466 (1997)
35. M.I. Chibisov, A.V. Roitman, Zh. Eksp. Teor. Fiz. **116**, 236 (1999) [JETP **86**, 735 (1999)]
36. J.W. Farley, W.H. Wing, Phys. Rev. A **25**, 2397 (1981)
37. B.B. Kadomtsev, M.B. Kadomtsev, Phys. Scripta **50**, 243 (1994)
38. B.B. Kadomtsev, *Dynamics and Information* (Uspekhi Fizicheskikh Nauk, Moscow, 1997)
39. S.T. Belyaev, private communication
40. M.B. Mensky, Usp. Fiz. Nauk. **168**, 1017 (1998) [Phys. Usp. **41**, 17 (1998)]